Proceedings of the 35th European Safety and Reliability & the 33rd Society for Risk Analysis Europe Conference
Edited by Eirik Bjorheim Abrahamsen, Terje Aven, Frederic Bouder, Roger Flage, Marja Ylönen
 Published by Research Publishing, Singapore.
doi: 10.3850/978-981-94-3281-3_ESREL-SRA-E2025-P1572-cd

Synthetic Monitoring Data Generation for Fault Detection in Wind Turbines

Luiz David Ricarte de Souza Custodio

Department of Mechanical Engineering, University of São Paulo, Brazil. E-mail: david_ricarte@usp.br

Arthur Henrique de Andrade Melani

Department of Mechatronics and Mechanical Systems Engineering, University of São Paulo, Brazil. E-mail: melani@usp.br

Welker Facchini Nogueira

Department of Mechatronics and Mechanical Systems Engineering, University of São Paulo, Brazil. E-mail: welkerfacchini@usp.br

Demetrio Cornilios Zachariadis

Department of Mechanical Engineering, University of São Paulo, Brazil. E-mail: dczachar@usp.br

Gilberto Francisco Martha de Souza

Department of Mechatronics and Mechanical Systems Engineering, University of São Paulo, Brazil. E-mail: gfmsouza@usp.br

The effective detection of faults in wind turbines is crucial to ensure their reliability and reduce downtime. However, the availability of real-world monitoring data representing various fault scenarios is often limited, making it difficult to test and validate fault detection algorithms. This paper presents a method for generating synthetic wind turbine monitoring data using OpenFAST, an open-source simulator developed by the National Renewable Energy Laboratory (NREL). The simulator is used to model the dynamic behavior of a wind turbine under both normal operating conditions and in a specific fault scenario, which is rotor unbalance. By leveraging OpenFAST's ability to simulate the physical response of a wind turbine to environmental conditions and mechanical faults, we can create a comprehensive dataset that mimics real-world monitoring data. This dataset covers various operating conditions, including different wind speeds and directions, enhancing the generalizability of the data for fault detection purposes. The generated data is intended to support the development and testing of fault detection tools, providing a benchmark for algorithms that rely on monitoring data to predict, detect, and diagnose failures in wind turbines. The synthetic dataset aims to fill the gap between theoretical models and real-world applications, facilitating the design of more robust and accurate fault detection methods. This study demonstrates the potential of using high-fidelity simulations for reliability analysis and underscores the value of synthetic data in advancing predictive maintenance strategies for renewable energy systems.

Keywords: Synthetic Data Generation, Fault Detection, Wind Turbines Monitoring, OpenFAST Simulation.

1. Introduction

The increasing reliance on renewable energy sources, such as wind power, has emphasized the need to ensure the reliability and operational efficiency of wind turbines. Operating under harsh environmental conditions, critical component failures in wind turbines can result in significant energy losses, high maintenance costs, and potential environmental impacts. Early fault detection through data-driven monitoring systems is essential to enhance reliability and reduce maintenance expenses.

Condition Monitoring Systems (CMS) play a vital role in identifying potential faults before they escalate into critical failures (Souza et al. 2022). However, a major challenge in developing effective predictive models is the limited availability of real failure data, as failures are relatively rare in well-designed and maintained turbines. This limitation underscores the importance of synthetic data generation to expand the datasets available for training and validating robust fault detection models.

Several studies have explored innovative approaches to synthetic data generation in the wind energy sector. For instance, hybrid digital twins have been developed to combine real operational data with physical models, generating synthetic datasets that simulate diverse fault conditions (Pujana et al. 2023). Similarly, synthetic SCADA datasets have been created to replicate gearbox failure scenarios, enhancing the robustness of fault detection systems (Milani et al. 2024). Generative adversarial networks (GANs) have been utilized to produce synthetic fault data, addressing the limitations of small sample sizes in wind turbine fault classification (Liu et al. 2019).

Data-driven approaches, such as GANs or other machine learning models, rely on the availability of real failure datasets for training, which can be a limiting factor when such data is scarce. In contrast, physics-based simulation models enable the generation of fault scenarios grounded in the fundamental principles of system dynamics, ensuring physically consistent results without the need for historical failure data.

This study proposes a novel methodology for generating synthetic monitoring data using the OpenFAST simulator (J. M. Jonkman and Buhl 2005). This methodology enables the creation of a comprehensive dataset that reflects real operational conditions, including simulated rotor unbalance failures under different wind and load scenarios.

2. The Proposed Method

Synthetic data generation demands the adoption of reliable and accessible simulation tools so the validity of the results can be confirmed by the scientific community. OpenFAST, an open-source simulation platform developed by NREL (J. M. Jonkman and Buhl 2005) to analyse the aeroelastic interactions between the wind and the turbine during the energy harvesting process is adopted to calculate the output variables that describe the dynamic behaviour of the wind generator. It is considered a benchmark computational code comprising a set of modules which enable the generation of wind profiles, the description of the structural stiffness, inertia and damping properties of the complete wind turbine model together with the definition of control strategies and parameters. To further facilitate the replication of the analyses results, a widely studied baseline 5MW turbine model also conceived by NREL (J. Jonkman et al. 2009) was chosen to exemplify the application of the proposed methodology.

It is important to note that, although OpenFAST was not originally developed to simulate the operation of wind turbines under faulty conditions, it is possible to do so by changing some of the software's input parameters so that the physical model represents the machine's operation under these conditions. Such changes, which constitute the novelty of this work, allow us to extrapolate the use of the software to generate synthetic data for monitoring wind turbines under faulty conditions. In this work, we will focus on changing the software's input parameters to simulate the operation of a turbine that presents an unbalance, a relatively common fault in this type of machine. In this chapter, section 2.1 presents a description of OpenFAST and its modules, section 2.2 shows the characteristics of the modeled and simulated wind turbine, section 2.3 describes the wind conditions considered in the simulations performed, and finally, section 2.4 presents the different levels of unbalance modeled for the simulations performed.

2.1. *Simulation Platform: OpenFAST Overview*

The OpenFAST software streamlines the simulation of wind-turbine interactions in energy extraction by providing a multiphysics tool combining aerodynamic and structural modeling. It integrates 15 modules, four of which were used to generate the synthetic data in this study.

The AeroDyn module evaluates aerodynamic performance by dividing blades into segments based on geometric properties (aerofoil profiles). Using Beam Element Momentum (BEM) Theory, it calculates lift, drag, and moments, incorporating corrections for axial and tangential induction and dynamic effects like stall delay and aerofoil dynamics (J. M. Jonkman and Buhl 2005).

The ElastoDyn module handles structural dynamics, analyzing the turbine's blades and tower under aerodynamic, gravitational, and centrifugal loads. Using beam elements with six degrees of freedom per node, it simulates the dynamic behavior of the turbine, including drivetrain torsional vibrations (J. M. Jonkman and Buhl 2005).

ServoDyn implements active control strategies for generator torque and blade pitch, optimizing energy capture below rated speed and maintaining constant rotor speed and power above rated speed up to 25 m/s (Fig. 1). It also simulates electrical systems, addressing power generation and grid interaction under extreme conditions (J. M. Jonkman and Buhl 2005).

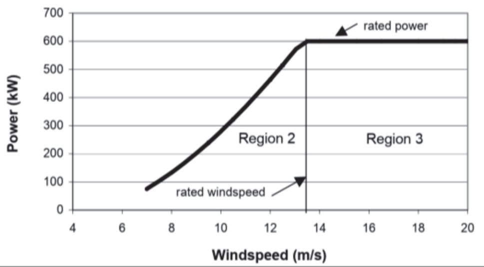

Fig. 1. Wind turbine power curve; region 2 features variable rotor speed controlled by generator torque; region 3 maintains constant drivetrain speed (Wright, 2004).

The InflowWind module couples wind models generated by TurbSim with OpenFAST, enabling simulations ranging from idealized wind profiles to complex turbulent environments (J. M. Jonkman and Buhl 2005). TurbSim, compliant with IEC 61400-1 standards (IEC 2019), generates three-dimensional turbulent wind grids that capture spatial and temporal fluctuations, enhancing the realism of wind turbine simulations (Churchfield et al. 2012). These grids are constructed using the Kaimal turbulence spectrum, which characterizes turbulence energy distribution across frequencies (Subramanian, Chokani, and Abhari 2016). Fig. 2 illustrates a turbine positioned within the wind grid.

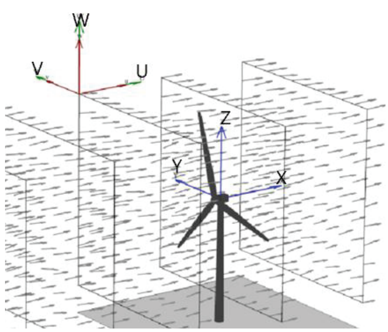

Fig. 2. Wind field generated by TurbSim (B. J. Jonkman 2009).

By integrating Large Eddy Simulation (LES) with sub-grid turbulence models, TurbSim refines the wind field for high-interaction regions while ensuring computational efficiency in downstream areas. This approach accurately simulates wind-turbine interactions, including the dynamic effects of wind on blades, towers, and nacelles.

2.2. *Wind Turbine Model*

The 5MW turbine baseline model made available by NREL was considered appropriate for this study due to its representative size and the easiness to compare and check the results of the simulations with those of previously published works; the gross properties of the baseline model are given in Table 1. Though this model was initially proposed for an offshore turbine, all the calculations assume the tower clamped onshore. A detailed description of the geometric, structural and inertia properties of the rotor (hub and blades), the nacelle and its components, the drivetrain and the tower is provided in (J. Jonkman et al. 2009).

Table 1. Gross properties of the 5MW turbine baseline model (J. Jonkman et al. 2009).

Property	Value
Rating	5 MW
Rotor Orientation, Configuration	Upwind, 3 Blades
Control	Variable Speed, Collective Pitch
Drivetrain	High Speed, Multiple-Stage Gearbox
Rotor, Hub Diameter	126 m, 3 m
Hub Heigth	90 m
Cut-in, Rated, Cut-Out Wind Speed	3 m/s, 11,4 m/s, 25 m/s
Rated Tip Speed	80 m/s
Overhang, Shaft Tilt, Precone	5 m, 5º, 2,5º
Rotor Mass	109,389.852 kg
Blade Mass	17,536.613 kg
Nacelle Mass	240,000 kg
Tower Mass	347,460.250 kg
Coordinate Location of Overall CM	(-0.2 m, 0.0 m, 64.0 m)

2.3. *Wind Conditions*

Three average wind speed values are enough to simulate representative normal operation conditions: 7m/s (generator torque control region - see Figure 1), 10,5 m/s (transition region) and 14m/s (above rated speed). Considering three turbulence levels, 12%, 14% and 16%, as described in IEC 61400-1 for standard wind turbine classes, results in nine combinations of wind parameters that cover a wide range of normal operating conditions

2.4. *Unbalance Levels*

To adopt representative real world acceptable residual unbalance levels, design guidelines from (IEC 2019) regarding ice formation will be followed.

According to the standard, 750 h of annual expected long-term rotor icing may be assumed for load calculations; in this context, the mass unbalance resulting from icing of the blades provides realistic load estimates to determine the range of unbalance values considered in the synthetic data generation. The ice mass distribution (mass / unit length) increases linearly from zero in the rotor axis to the maximum value at the rotor tip and the ice load distribution is calculated as shown in Eq. (1) (IEC 2019):

$$M(r) = A \times C_{85\%} \times r \tag{1}$$

where M(r) is the mass distribution on the leading edge of the rotor blade [kg/m], A is 0.125 [kg/m3], $C_{85\%}$ is the chord length at 85% rotor radius [m], and r is the radial position from rotor axis (hub centre) [m]. Blade aerodynamic properties of the 5MW baseline turbine are presented in (J. Jonkman et al. 2009); thus, 85 % of a 63 m rotor radius corresponds to ~54m, which, indicates an aerofoil section placed between nodes 14 and 15 (airfoil NACA64), resulting in $C_{85\%}$~2.5m. From Eq. (1) the total ice mass amounts to 621kg and its mass centre is located 42m from the rotor axis; these results are consistent with previous ones regarding a much smaller turbine model Senvion MM92 CCV with 2.05 MW rated power, 80 m hub height and 92 m rotor diameter (Rissanen et al. 2016)

For ultimate load analysis, ice mass formation on two blades and aerodynamic penalties on all rotor blades should be investigated, according to (IEC 2019). A simple calculation using the previous results shows that the corresponding rotor mass centre is located ~0.24m from the hub centre (Obs.: the result negligibly changes if one adopts icing on a single blade). For fatigue analysis, ice mass on all rotor blades except one rotor blade where 50% of the ice mass should be considered, in addition to aerodynamic penalties on all rotor blades, should be investigated; this results in a ~11.7cm rotor mass eccentricity. Since this study does not include aerodynamic penalties, considering only the effects of mass unbalance yields a less severe loading condition, which means that an even higher level of mass unbalance could be necessary to reach the same loads.

It is noteworthy that this level of residual unbalance is considerably higher than the ones adopted in previous studies which consider unbalance quality scale G of ISO 21940-11:2016 standard (ISO 2016) in accordance to (Kusnick, Adams, and Griffith 2015). Nevertheless, ISO 21940-11 standard does not cover rotation values below 20 rpm; for such very slow machines the permissible residual specific unbalance "eper" ranges between ~10,000 and ~100,000 [g.mm/kg] according to field common experience (see ISO 21940-11, Figure 2, pg.9 (ISO 2016)). Thereby, extrapolations show that the corresponding permissible residual unbalance for a ~110,000 kg rotor rotating at 12,1rpm could be defined between ~1,650 and ~66,000 [kg.m]. For instance, the previously calculated 621kg ice mass located 42m from the rotor axis results in a residual unbalance of ~26,100 kg.m which may be compatible with the operational conditions of a wind turbine properly designed.

Based on field observations, one of the most common causes of blades failures arises from mass losses close to their tips due to lightning strikes (Katsaprakakis, Papadakis, and Ntintakis 2021). In this context, three different levels of mass unbalance resulting from mass losses near blade tips are herein adopted to simulate unbalanced operation; Table 2 describes the percentages of blade mass loss and rotor mass related properties.

The 1% blade mass loss yields a loading condition similar, though milder, to the one considered in the fatigue analysis of iced rotors described above, and results in a centrifugal force of ~17.63 kN, which corresponds to 1.64% of the rotor weight; this unbalance causes a small magnitude load fluctuation. The other two unbalance levels corresponding to 3% and 5% blade mass losses are classified as medium and severe, respectively.

Combining the nine wind conditions described in Section 2.3 with the three unbalance levels shown in Table 2 one gets a set of 27 unbalanced rotor operation conditions. In total, therefore, 36 different simulations were performed:

9 representing the turbine behavior without unbalance in each of the different wind conditions, and 27 with unbalance.

Table 2. Percentage of blade mass loss and rotor residual unbalance (blade mass original value: 17,536.62 kg).

Percentage of blade mass loss	Resulting blade mass (kg)	Resulting rotor mass (kg)	Resulting rotor mass centre excentricity (cm)	Rotor residual unbalance (kg.m)	ISO G quality grade* (mm/s)
1%	17,361.30	109,824.60	10.0	~11,000	127
3%	17,010.50	109,473.90	30.3	~33,200	382
5%	16,659.80	109,123.20	50.6	~55,200	636

*G (quality grade) is calculated using the expression $U_{per} = 9.549 \cdot G \cdot m/n$ (mm/s) (ISO 2016), with U_{per} being the adopted rotor permissible residual unbalance, m being the rotor mass (kg) and n being the nominal speed (rpm).

3. Results

OpenFAST provides a variety of outputs that allow for detailed analysis of structural, aerodynamic, control, and even hydrodynamic phenomena (for offshore turbines). Among the main variables available are forces and moments at the blade roots (e.g., RootMzb1), displacements and accelerations in components such as the tower (e.g., TwrBsMyt, TwrBsAcc), and vibrations in components such as the rotor shaft and nacelle (e.g., LSSTipMxa, NcIMUTAxs).

OpenFAST calculates these variables using coupled models that integrate the AeroDyn, ElastoDyn, and ServoDyn modules. In this study, considering the simulation of mass unbalance in the turbine blades, nacelle vibrations were selected as the primary variables for analysis. The selected variables are:

- NcIMUTAxs: Translational acceleration along the nacelle's X-axis. This variable is particularly important for identifying longitudinal movements resulting from the mass unbalance.
- NcIMUTAys: Translational acceleration along the nacelle's Y-axis, used to monitor lateral vibrations of the nacelle.
- NcIMUTAzs: Translational acceleration along the nacelle's Z-axis, which provides information about vertical vibrations and their possible impacts on the structure.

These variables are calculated by OpenFAST based on the displacements and forces applied to the nacelle due to the unbalance and can be monitored alongside data from Condition Monitoring Systems (CMS), which are used for structural condition analysis and fault detection in wind turbines. The integration between OpenFAST-simulated data and CMS-collected data allows for cross-validation of results and potential applications in predictive maintenance practices. Analyzing these variables is essential, as mass unbalance can amplify nacelle vibrations, leading to effects such as premature wear of components and increased dynamic loads on the structure, ultimately impacting the turbine's service life.

The dynamic behavior of the turbine is thoroughly described by a large set of time series comprising its power production, forces and moments acting on the blades, drivetrain, nacelle and tower, blade tips displacements, nacelle accelerations, etc. For illustrative purposes only, Figures 4 and 5 present some of these results related to turbine operation under normal conditions and with the unbalanced rotor.

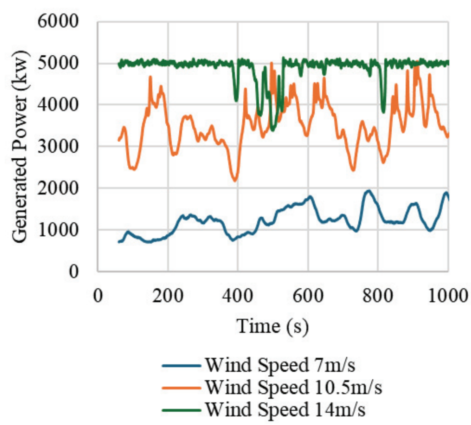

Fig. 3. Power production time series under normal operation conditions

To demonstrate that the proposed method is capable of correctly simulating the behavior of the wind turbine when there is an unbalance in its blades, the data simulated via OpenFAST were analyzed through a Fast Fourier Transform (FFT). The FFT allows Nacele vibration data to highlight the change in the behavior of the machine when it is unbalanced. The FFT is widely used for fault detection and condition monitoring of industrial equipment (Wang and Gao 2006; Randall 2011).

The analysis was carried out in a Python environment using the NumPy and pandas libraries, which enable efficient manipulation of large data sets. The FFT was applied using the SciPy library. This ecosystem of tools ensures reproducibility, scalability, and straightforward handling of large-volume time series, making it possible to tailor the analysis process to data demands and the hypotheses being investigated.

The main objective of using the FFT is to extract attributes representative to the turbine's vibratory behavior. To achieve this, the methodological strategy adopted includes:

(i) Temporal segmentation of the signal;
(ii) Application of the Fast Fourier Transform (FFT);
(iii) Calculation of statistical metrics in the time domain.

Initially, the data was segmented into time windows to preserve the system's dynamic evolution and facilitate the identification of specific events. Subsequently, the FFT was applied, a technique that decomposes the signal into its spectral components, enabling the recognition of critical frequencies associated with rotation harmonics and potential mechanical faults, such as unbalance, misalignment, and backlash (Randall 2011). The spectral components derived from the FFT highlight frequencies of interest linked to turbine rotation, mechanical coupling, and potential external excitations (Randall 2011).

The OpenFAST simulation provided data sampled at 25 Hz. To obtain characteristics that capture the temporal evolution of the system and still maintain adequate spectral resolution, the signal was segmented into two-minute windows, yielding blocks of 3,000 samples (Oppenheim and Schafer 2009; Bendat and Piersol 2010). Each segment was treated independently to extract the attributes.

Fig. 4 shows the original vibration signal measured over a time window of 120 seconds in the Nacelle acceleration signal on the X axis (NcIMUTAx). The horizontal axis shows the time in seconds, while the vertical axis represents the instantaneous amplitude of the signal. Fig. 5 shows the result of the Fast Fourier Transform (FFT) applied to the same signal shown above in the time domain, now converting the oscillations as a function of frequency. The horizontal axis shows the frequencies in hertz (Hz), while the vertical axis indicates the magnitude (or spectral amplitude) of the signal at each frequency. Low-rotation vibration analysis makes it possible to detect specific anomalies, such as unbalance or variations in wind load, which can be reflected in additional peaks or increases in amplitude close to the fundamental frequency.

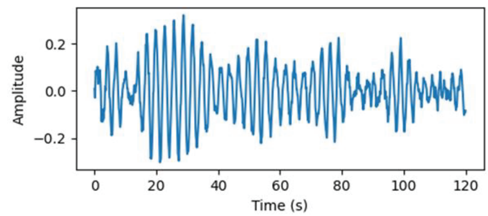

Fig. 4. Original signal from NclMUTAxs

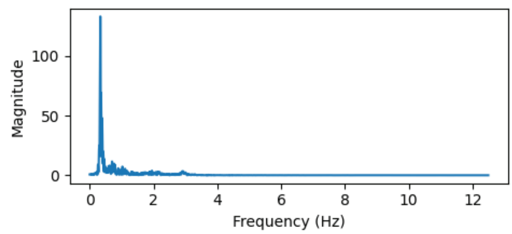

Fig. 5. Result of the FFT applied to NclMUTAxs

The FFT of each time window converts the signal from the time domain to the frequency domain, thereby facilitating the identification of harmonic peaks associated with faults and specific dynamic behaviors (Inman 2014). For real signals, the spectrum is symmetric about zero; hence, only the positive frequency portion is analyzed (Bendat and Piersol 2010).

For the three vibration variables, the FFT was applied to convert the signals from the time domain to the frequency domain every 120 seconds. But it is important to note that unbalance in a rotating machine causes changes in a specific region of the FFT graph: it causes an increase in the magnitude recorded at the frequency corresponding to the machine's rotation frequency. This implies that, in the specific case of unbalance, it is necessary to observe only a specific point of each of the generated graphs. This provides essential information for interpreting phenomena related to the dynamic behavior of the machine and for identifying early signs of mechanical faults in rotating machinery (Randall 2011).

Since the machine's rotation is not fixed, however, an average of the magnitude values around the mean rotation value observed in the 120 seconds was used in this work. More specifically, after obtaining the mean (u) and standard deviation (p) of the machine's rotation for a given time window of 120 seconds, the interval between u - p and $u + p$ in the FFT graph was considered and the average of the magnitudes observed within this interval in the graph was calculated. This approach ensures that the spectral analysis remains focused on the band most pertinent to the unbalanced rotor's dynamics.

Fig. 6 shows the results obtained by extracting this value from each FFT plot obtained over 50 minutes for the four conditions analyzed (normal operation, 1%, 3%, and 5% of unbalance) for the NclMUTAxs variable. The results show that an unbalance in the machine does not promote a change in the way the machine vibrates along the nacelle's X-axis. However, when observing Fig. 7, which shows the result obtained for the NclMUTAys variable, it is noted that the unbalance has a clear effect on the vibration of the turbine along the nacelle's Y-axis. The results obtained show that the unbalance was successfully simulated by OpenFAST and that the synthetic data obtained can represent the behavior of the machine when it presents this fault. Furthermore, the results are in perfect agreement with previously theoretical and experimental ones published up to now, especially regarding the dependence between the magnitude of the 1x rotation FFT harmonic and rotor speed (Askari et al. 2024).

4. Conclusions

This study demonstrates the potential of OpenFAST simulations for generating synthetic monitoring data under fault conditions in wind turbines. By simulating rotor unbalance scenarios, the research provides insights into the dynamic behavior of turbines. Future work will focus on simulating a broader range of wind turbine failures using OpenFAST, including gear and generator malfunctions, under varying environmental conditions. Additionally, the data produced through these simulations will be compiled into a publicly accessible database, enabling researchers and industry professionals worldwide to develop and validate fault detection algorithms.

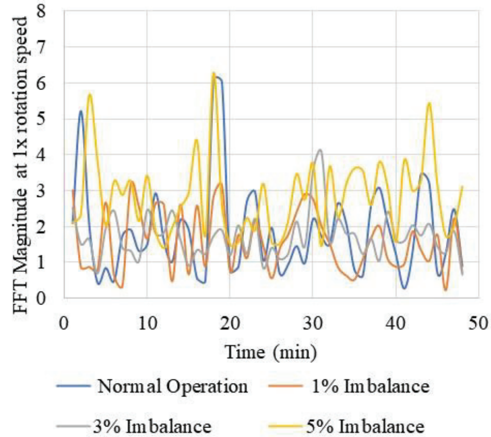

Fig. 6. Results of the FFT magnitude at 1x rotation speed applied to NclMUTAxs

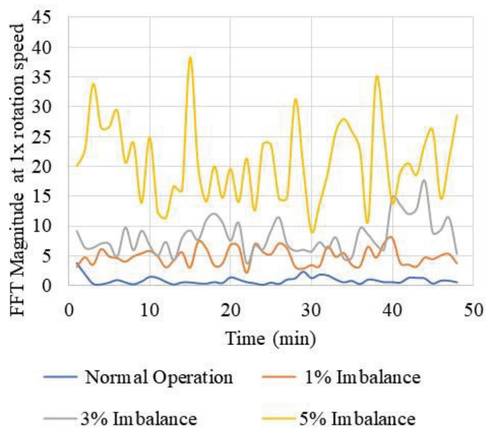

Fig. 7. Results of the FFT magnitude at 1x rotation speed applied to NclMUTAys

Acknowledgement

We gratefully acknowledge the support of the RCGI – Research Centre for Greenhouse Gas Innovation (23.1.8493.1.9), hosted by the University of São Paulo (USP), sponsored by FAPESP – São Paulo Research Foundation (2020/15230-5), and sponsored by TotalEnergies, and the strategic importance of the support given by ANP (Brazil's National Oil, Natural Gas and Biofuels Agency) through the R\&DI levy regulation.

References

Askari, Amir R., Len Gelman, Russell King, Daryl Hickey, and Andrew D. Ball. 2024. "A Novel Diagnostic Feature for a Wind Turbine Imbalance Under Variable Speed Conditions." *Sensors* 24 (21): 7073. https://doi.org/10.3390/s24217073.

Bendat, Julius S., and Allan G. Piersol. 2010. *Random Data*. Wiley. https://doi.org/10.1002/9781118032428.

Churchfield, Matthew J., Sang Lee, John Michalakes, and Patrick J. Moriarty. 2012. "A Numerical Study of the Effects of Atmospheric and Wake Turbulence on Wind Turbine Dynamics." *Journal of Turbulence* 13 (January):N14. https://doi.org/10.1080/14685248.2012.668191.

IEC. 2019. "IEC 61400-1 Wind Energy Generation Systems – Part 1: Design Requirements." Geneva, Switzerland.

Inman, Daniel J. 2014. *Engineering Vibration*. 5th ed. New York: Pearson.

ISO. 2016. "ISO 21940-11:2016 Mechanical Vibration — Rotor Balancing Part 11: Procedures and Tolerances for Rotors with Rigid Behaviour." Geneva, Switzerland.

Jonkman, B. J. 2009. "Turbsim User's Guide: Version 1.50." Golden, CO (United States). https://doi.org/10.2172/965520.

Jonkman, J., S. Butterfield, W. Musial, and G. Scott. 2009. "Definition of a 5-MW Reference Wind Turbine for Offshore System Development." Golden, CO. https://doi.org/10.2172/947422.

Jonkman, J. M., and M. L. Jr. Buhl. 2005. "FAST User's Guide - Updated August 2005." Golden, CO. https://doi.org/10.2172/15020796.

Katsaprakakis, Dimitris Al., Nikos Papadakis, and Ioannis Ntintakis. 2021. "A Comprehensive Analysis of Wind Turbine Blade Damage." *Energies* 14 (18): 5974. https://doi.org/10.3390/en14185974.

Kusnick, Josh, Douglas E. Adams, and D. Todd Griffith. 2015. "Wind Turbine Rotor Imbalance Detection Using Nacelle and Blade Measurements." *Wind Energy* 18 (2): 267–76. https://doi.org/10.1002/we.1696.

Liu, Jinhai, Fuming Qu, Xiaowei Hong, and Huaguang Zhang. 2019. "A Small-Sample Wind Turbine Fault Detection Method With Synthetic Fault Data Using Generative Adversarial Nets." *IEEE Transactions on Industrial Informatics* 15 (7): 3877–88. https://doi.org/10.1109/TII.2018.2885365.

Milani, Ali Eftekhari, Donatella Zappalá, Francesco Castellani, and Simon Watson. 2024. "Boosting Field Data Using Synthetic SCADA Datasets for Wind Turbine Condition Monitoring." *Journal of Physics: Conference Series* 2767 (3): 032033. https://doi.org/10.1088/1742-6596/2767/3/032033.

Oppenheim, Alan V., and Ronald W. Schafer. 2009. *Discrete-Time Signal Processing*. 3rd ed. Upper Saddle River: Pearson.

Pujana, Ainhoa, Miguel Esteras, Eugenio Perea, Erik Maqueda, and Philippe Calvez. 2023. "Hybrid-Model-Based Digital Twin of the Drivetrain of a Wind Turbine and Its Application for Failure Synthetic Data Generation." *Energies* 16 (2): 861. https://doi.org/10.3390/en16020861.

Randall, Robert Bond. 2011. *Vibration-based Condition Monitoring*. Wiley. https://doi.org/10.1002/9780470977668.

Rissanen, Simo, Ville Lehtomäki, Jani Wennerkoski, Matthew Wadham-Gagnon, and Klaus Sandel. 2016. "Modelling Load and Vibrations Due to Iced Turbine Operation." *Wind Engineering* 40 (3): 293–303. https://doi.org/10.1177/0309524X16645484.

Souza, G. F. M., A. Caminada Netto, A. H. A. Melani, M. A. C. Michalski, and R. F. da Silva. 2022. *Reliability Analysis and Asset Management of Engineering Systems*. Elsevier. https://doi.org/10.1016/C2020-0-00478-0.

Subramanian, B., N. Chokani, and R.S. Abhari. 2016. "Aerodynamics of Wind Turbine Wakes in Flat and Complex Terrains." *Renewable Energy* 85 (January):454–63. https://doi.org/10.1016/j.renene.2015.06.060.

Wang, Lihui, and Robert X. Gao. 2006. *Condition Monitoring and Control for Intelligent Manufacturing*. Edited by Lihui Wang and Robert X. Gao. London: Springer London. https://doi.org/10.1007/1-84628-269-1.

Wright, A D. 2004. "Modern Control Design for Flexible Wind Turbines." Golden, CO (United States). https://doi.org/10.2172/15011696.